

Conductivity and Hall Effect of ZnO at Low Temperatures*†

SOL E. HARRISON‡

Physics Department, University of Pennsylvania, Philadelphia, Pennsylvania

(Received May 20, 1953; revised manuscript received June 25, 1953)

The Hall effect and conductivity of zinc oxide have been measured in dense polycrystalline samples and two single crystals.

It has been found that the usual simple Wilson semiconductor model is inadequate for the proper interpretation of results. Several modifications and additions have been suggested for the usual single-level impurity semiconductor. Allowance has been made for the polycrystalline nature of the sintered specimens in deducing the bulk properties.

Three models are successful in giving the correct interpretation for the experimental results of the Hall curves. These are: (1) orbital degeneracy of electrons attached to an interstitial zinc atom; (2) additional energy levels at traps at the impurity level, where the number of traps is much greater than the number of donors; (3) traps far below the donor level that greatly out-

number the donors [this is mathematically the same as (2) but necessitates other lattice imperfections for physical realization].

Physical realization of these energy level schemes is considered in the light of the other physical properties of ZnO, such as luminescence and photoconductivity. These physical models are examined with the aid of present-day knowledge of the alkali halides and other ionic crystals. It is found that pairs of positive (zinc) plus negative (oxygen) ion vacancies with excess oxygen ion vacancies are capable of reproducing the diversified electrical and optical properties of zinc oxide semiconductor. The previous scheme of frozen-in interstitial zinc atoms is shown to be incompatible with our experimental results. Experiments are proposed for further verification of the proposed model.

I. INTRODUCTION

ELECTRICAL measurements have been made on densely sintered zinc oxide samples and two single-crystal specimens. Resistivity and Hall coefficient measurements have been made over the temperature range from 54°K to 300°K. The sintered ZnO is believed to derive its extrinsic semiconductor properties from an excess of zinc created by the loss of oxygen in the sintering process. The single crystals¹ were formed accidentally, and we had no part in determining their physical properties. The data are analyzed to determine the variation of the concentration of current carriers and mobility with temperature. The results are interpreted in terms of existing theories of semiconduction.

1. Energy Levels in Zinc Oxide

ZnO has the wurtzite structure with a c/a ratio = 1.60² instead of the value 1.633 for a perfect hexagonal close-packed lattice. The specific gravity of ZnO is 5.68, and its fusing point is about 1975°C.³ The static dielectric constant is approximately 12, whereas the index of refraction is 2. The conductivity is generally a function of the heat treatment of the sample.

ZnO is an n -type semiconductor. This is due to the excess zinc in the lattice.⁴ The optical properties have

been reported by a number of authors.⁴⁻¹⁰ This compound exhibits photoconductivity in the range 2000A to 7000A. There is a sharp increase in photoresponse at about 3.2 ev which coincides with the onset of the absorption of light. This energy is assumed to be the long wavelength edge of the intrinsic absorption corresponding to the electronic transition from the top of the filled band¹⁰ to the bottom of the conduction band or to an exciton level close to the conduction band.

Electrical conductivity measurements of ZnO at low temperatures can generally be described by the theoretically well-founded relation:

$$\sigma = A \exp - (B/kT). \quad (I-1)$$

The values of A and B vary over wide ranges among the various observers who have measured thin films,¹¹⁻¹³ sintered specimens,^{11,14,15} and single-crystal samples.^{11,15} The relation between A and B has been discussed by Meyer¹⁶ and Busch.¹⁷ B is equal to $E_D/2$, where E_D is

⁵ E. Mollwo and F. Stöckmann, *Ann. Phys.* **3**, 240 (1948).

⁶ E. Mollwo, *Reichsber Physik* **1**, 1 (1944).

⁷ P. H. Miller, *Proceedings of the Conference of Semiconducting Materials* (Butterworths Publishing Company, London, 1951), p. 172.

⁸ E. Mollwo, *Z. Phys. Chem.* **198**, 298 (1951).

⁹ D. Warschauer, Technical Report No. 2, University of Pennsylvania, Jan. 25, 1952 (unpublished).

¹⁰ This is generally thought to be the O^{--} band. [See F. Seitz, *The Modern Theory of Solids* (McGraw-Hill Book Company, Inc., New York, 1940), p. 448.] However, J. H. DeBoer and E. J. W. Verwey [*Proc. Phys. Soc. (London)* **49**, 59 (1937) (extra part)] have suggested that the filled band is the $3d Zn^{++}$ band; for they point out that the metallic oxides with incomplete $3d$ states do not show photoconductivity while the oxides of the metals such as zinc with complete $3d$ shells do show a photoresponse.

¹¹ O. Fritsch, *Ann. Physik* **22**, 375 (1935).

¹² F. Stöckmann, *Z. Physik* **127**, 563 (1950).

¹³ K. Intemann and F. Stöckmann, *Z. Physik* **131**, 10 (1951).

¹⁴ P. H. Miller, Jr., *Phys. Rev.* **60**, 890 (1941).

¹⁵ E. E. Hahn, *J. Appl. Phys.* **22**, 855 (1951); Technical Report No. 17, University of Pennsylvania, U. S. Bureau of Ships Contract, October 31, 1949 (unpublished).

¹⁶ W. Meyer and H. Neldel, *Z. Tech. Phys.* **18**, 580 (1930).

¹⁷ G. Busch, *Helv. Phys. Acta* **19**, 189 (1946).

* The essential portion of a dissertation in physics presented to the faculty of the Graduate School of the University of Pennsylvania in partial fulfillment of the requirement for the degree of Doctor of Philosophy. A more extensive account of this work was given in Technical Report No. 3, June 30, 1952 (unpublished), copies of which can be obtained from P. H. Miller, Jr., Physics Department, University of Pennsylvania, Philadelphia, Pennsylvania.

† Supported in part by U. S. Office of Naval Research.

‡ Now at Eckert-Mauchly Division, Remington Rand, Inc., Philadelphia, Pennsylvania.

¹ We are indebted to Mr. E. Burstein of the Naval Research Laboratory and Mr. R. Ammon of the American Zinc Company for the single crystals.

² C. W. Bunn, *Proc. Phys. Soc. (London)* **47**, 835 (1935).

³ E. N. Bunting, *J. Research Natl. Bur. Standards* **4**, 131 (1930).

⁴ E. Mollwo and F. Stöckmann [*Ann. Phys.* **3**, 223 (1948)] have found excess zinc in their samples by chemical analysis.

the ionization energy of a donor,¹⁸ if we consider the single-level impurity semiconductor model as proposed by Wilson. The donors have generally been assumed to be interstitial excess zinc atoms. However, Stöckmann¹² believes he has evidence for donors in the form of oxygen ion vacancies as well as interstitial zinc. For dense sintered samples,^{14,15} E_D in the low-temperature region is of the order of 0.05 ev. The energy-level scheme is sketched in Fig. 1.

2. Preparation of Samples

Spectroscopically pure ZnO¹⁹ powder was pressed in the form of a cylinder in a multisectioned die, 0.566 in. in diameter, to a length of $\frac{1}{2}$ to 1 in. at a pressure of 7000 lb per inch.² These cylinders were sintered for 18 hours at temperatures varying from 900–1350°C. They were extracted from the furnace at various points on the cooling curve and quenched in air. The initial rate of heating had no effect on the electrical properties. The effects of the cooling rate and sintering temperature will be discussed under experimental results. From these sintered cylinders the samples used for measurement were cut in the form of flat rectangular slices; typical dimensions were 2 cm×0.5 cm×0.15 cm. Electrical contacts to the ZnO were made by first nickel plating and then soldering to the nickel plate.

3. Experimental Procedure

The fundamental experimental data obtained in this investigation were the temperature dependence of the Hall coefficient and the conductivity for various ZnO samples. The low temperature was obtained with the use of liquid oxygen. The temperature was measured by a Leeds and Northrup Type 8164 platinum resistance thermometer. The sample and thermometer were fastened to a copper block, and this ensemble was placed inside a copper can. All measurements, except the Hall voltage, were read with a Leeds and Northrup Type K potentiometer. After the misalignment voltage had been bucked out, the Hall voltage was read on a Leeds and Northrup dc microvoltmeter having a sensitivity of 1 microvolt per scale division. Magnetic fields of the order of 5000 gauss were used. Sample currents were 1 ma or less. The Hall voltage was a linear function of the field and sample current up to magnetic fields of 15 000 gauss and sample currents large enough to cause Joule heating.

¹⁸ Energy schemes where $E_D=B$ will be considered later.

¹⁹ Purchased from New Jersey Zinc Company, Palmerton, Pennsylvania.

Representative analysis:

Loss at 110°C	0.12%	Ca	0.003%
SO ₃	0.01	Na	0.003
H ₂ O sol. salts	0.05	Mg	0.0003
PbO	0.0005	Si	0.0003
As ₂ O ₃	0.000004	Fe	0.0008
Insol. in HCl	less than 0.01	Cu	0.0004
CdO	less than 0.003	Mn	0.0002
Al	less than 0.003		

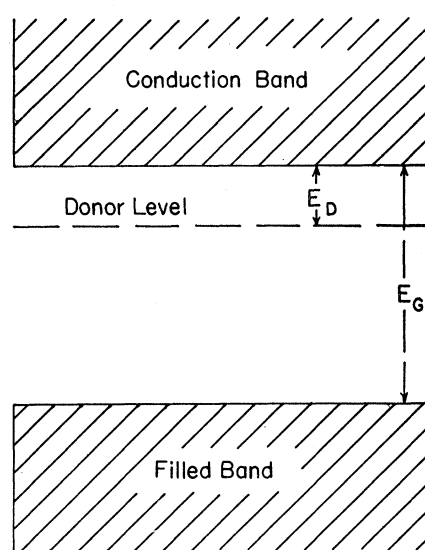


FIG. 1. Simple Wilson semiconductor model.

II. EXPERIMENTAL RESULTS

1. Sintered Samples of Moderate Heat Treatment

In this section we shall first examine the results of the measurements of the sintered samples of moderate heat treatment. Here "moderate" will designate the quenching treatment of the samples and refer to those samples quenched from temperatures up to 600°C. All samples were at the maximum sintering temperature (varying from 900°C to 1350°C) for a period of 18 hours.

The interpretation of conductivity measurements of polycrystalline semiconductors is, in general, open to some question due to the complicating action of grain boundaries, localized space charges, nonhomogeneity, etc. The exact consequences of grain structure and intergranular barriers on the Hall coefficient have as yet not been determined. It can be shown that a Hall measurement is characteristic of the bulk material when the grain boundary layer has a higher resistivity and is much thinner than the interior of the grain.¹⁵ Small good conducting point contacts between grains also give to the first approximation a Hall voltage characteristic of bulk material. Therefore, we feel that the Hall coefficient measurements give a somewhat more reliable description of the properties of the semiconductor and will discuss them in more detail than the conductivity measurements.

For all samples of moderate heat treatment, the experimental results of the measurement of Hall coefficient R are found to be similar. The number of charge carriers or impurity centers is, therefore, seen to be almost independent of the sintering and quenching temperatures within the limits mentioned above. The slopes of a $\ln R$ vs $1/T^\circ K$ for the straight line portion of the curves have values about 0.02 ev. Two of these Hall

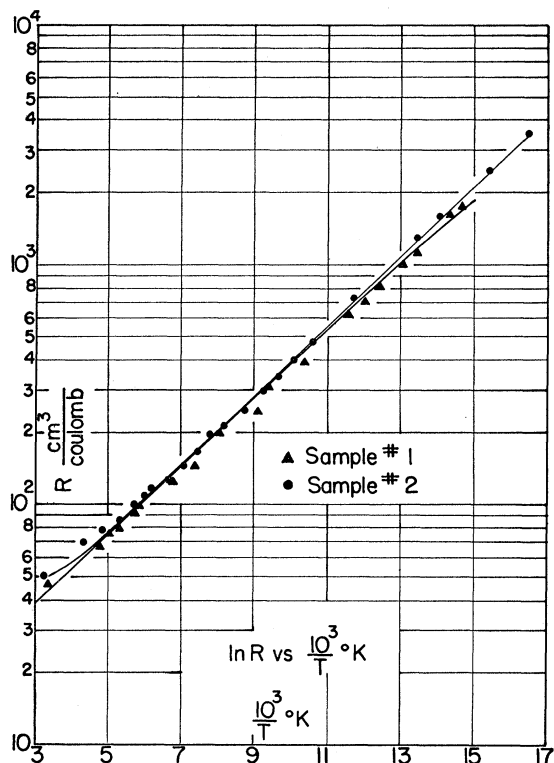


Fig. 2. Typical curves for Hall coefficient vs $1/T^{\circ}\text{K}$ for samples of "moderate" heat treatment. The results are apparently independent of heat treatment. Sample No. 1 was sintered at 1325°C and sample No. 2 at 1050°C for 18 hr.

curves are given in Fig. 2 and are typical of all of the samples of moderate heat treatment. These values of R correspond to about 10^{17} charge carriers/cm³ at room temperature according to the equation

$$R = (3\pi/8)(1/ne), \quad (\text{I-2})$$

where n = the concentration of electrons in the conduction band, e = the electronic charge in coulombs, and R is given in cm³/coulomb. The expression for n is

$$n = 7.4 \times 10^{18}/R. \quad (\text{I-3})$$

Though the conductivity (σ) has practically the same temperature dependence from sample to sample, the values measured at any one temperature may vary by a factor of 100 from sample to sample. The straight line portion of $\ln \sigma$ vs $1/T^{\circ}\text{K}$ has a slope of the value of 0.02 eV for all samples. Figure 3 shows the conductivity plots for the same two samples.²⁰ These curves demonstrate maxima at about 200°K . The maxima exhibited by these curves indicate that the number of electrons in the conduction band is approaching the saturation value while the mobility is decreasing rapidly as T increases.

In Fig. 4 we have plotted the mobility b curves of samples 1 and 2. It can be seen that the two mobility

²⁰ No. 1 was sintered at 1325°C , and No. 2 at 1050°C .

curves have practically the same temperature dependence. The mobilities of these sintered samples at room temperature lie between the values of 6 and 65 cm²/v sec. (Mobility b equals $R\sigma$.) The maximum value of the mobility obtained as the temperature is lowered is roughly three times that at room temperature. It should be noted that the mobility is temperature independent from 160° down to 54°K . Figure 4 indicates that the mobility is affected by the sintering temperature. X-ray measurements reveal that the grain size increases as the sintering temperature is raised. Assuming a preferential growth of the crystallites, we can expect just this variation in curves of mobility if the mobility along one axis of the crystal is greater than along the second axis. Single crystals of ZnO exhibit a conductivity ratio between 4 and 10^{21} to 1 at room temperature, i.e., σ parallel to the c axis is 4 to 10 times as large as σ perpendicular to the c axis. Preliminary microscopic examination does not indicate preferential growth. This interpretation is not unique since, if one considers Hahn's¹⁵ model of the bulk ZnO surrounded by layers of different stoichiometric composition of ZnO, the displacement of the mobility curves as shown in Fig. 4 might also be interpreted as an indi-

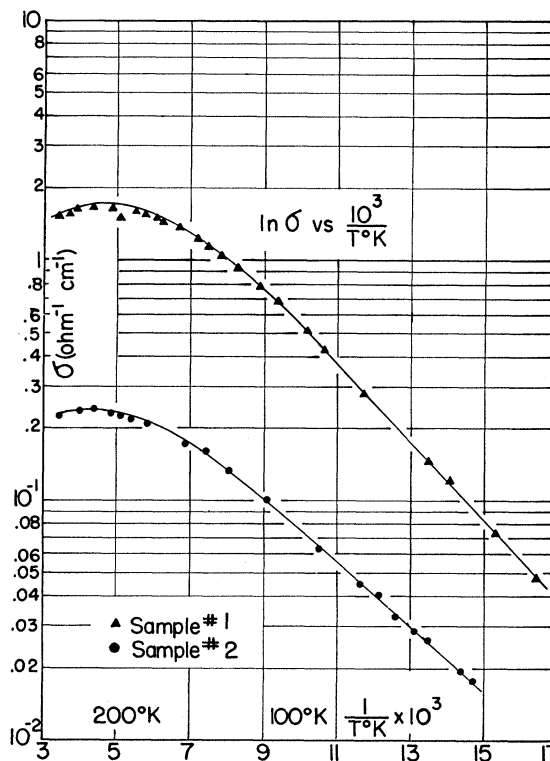


Fig. 3. Conductivity curves for samples No. 1 and No. 2. Heat treatment does affect the conductivity, but the slope remains constant.

²¹ This range in values is due to the fact that in the a direction in a tiny hexagonal crystal of ZnO it is very difficult to obtain accurate conductivity measurements.

cation that the conductivity of both regions is the same function of T . Also, if we assume a model of grains held together by narrow necks of identical material, the conductivity of the necks would be the same function of the temperature as the main body of the grain.

2. Measurements on Other Samples

A. Single Crystals

Measurements of conductivity and Hall effect have also been made on two single crystals of ZnO in the region 54°K to 300°K. The results of these measurements are shown in Figs. 5, 6, and 7.

Sample *A* had a yellowish-green coloration while sample *B* was almost colorless with a slight trace of yellow. A companion crystal of *B* was found to be spectroscopically pure. We had only one crystal of the *A* variety, and chemical analysis was not made. Both samples were quite transparent. Pure ZnO would be colorless because the intrinsic absorption begins at 3900Å.

The plots of the Hall effect for both samples indicate that the slopes are the same as that of the sintered samples considered in Sec. II.1. Also, these curves demonstrate a decreasing slope at the lower end of the temperature range, indicating the possible effect of the impurities that produce the coloration of the crystals. The conductivity curve for sample *A* is very similar to

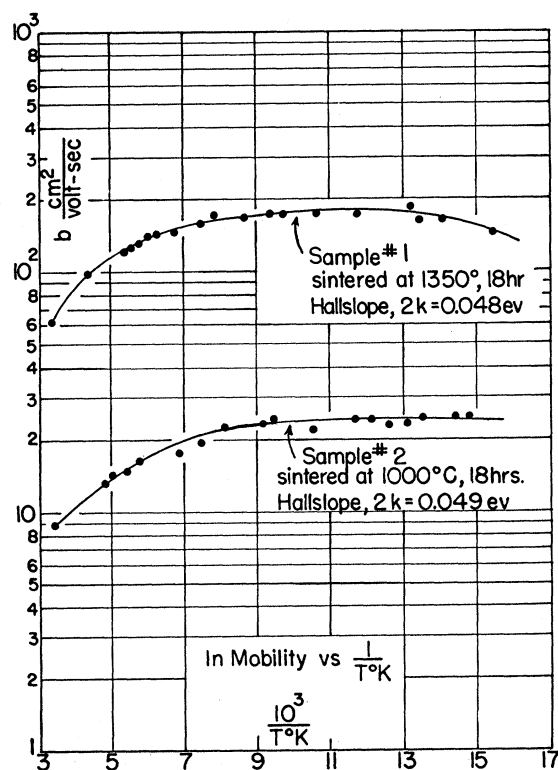


FIG. 4. Mobility vs $1/T^{\circ}\text{K}$ for samples No. 1 and No. 2. The curves have the same temperature dependence. The mobility for low temperatures is independent of temperature.

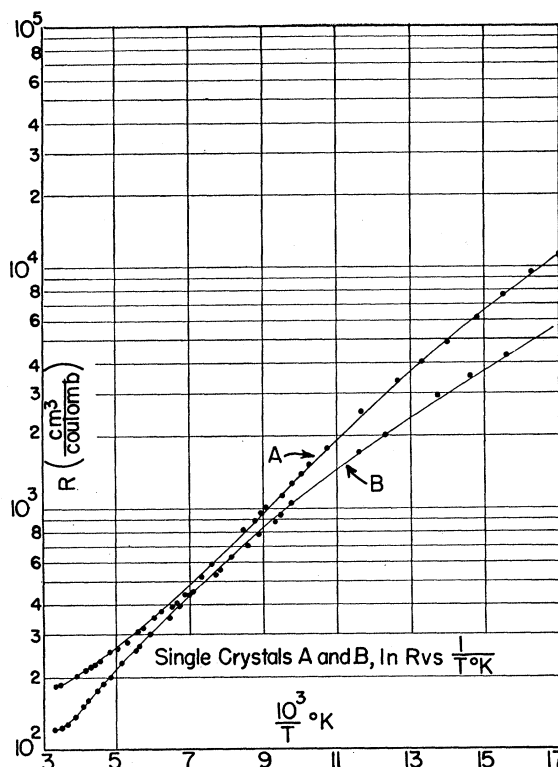


FIG. 5. Single crystals *A* and *B*, Hall coefficient vs absolute reciprocal temperature. The Hall curves of single crystals are very similar to polycrystalline samples.

that of the sintered specimens with the conductivity peak appearing about 160°K, which is at a somewhat lower temperature than the peaks of the sintered samples. For crystal *B* the conductivity exhibits no peak, and we find a curve that is somewhat more irregular than the usual conductivity plot. There is also an apparent increase in slope with increase in temperature. This behavior is not reflected in Hall effect measurements.

The mobility calculated as a product of R and σ gives a curve for sample *A* that is similar to the curves of Fig. 4. The mobility of sample *B* demonstrates a rather anomalous behavior. See Figs. 5-7.

B. Other Sintered Samples

Samples have been quenched by removing them from the oven at the sintering temperature. These samples exhibit a room temperature conductivity 10^{-2} to 10^{-3} times that of the previously discussed samples. The Hall coefficient is roughly 10 times as large. A temperature dependence of the Hall coefficient is difficult to obtain because of large drifts and extraneous voltage pulses appearing across the Hall probes. A conductivity-temperature plot reveals no conductivity peak (Fig. 8) and has a form similar to that of crystal *B*. Between 54°K and 90°K the slope is 0.03 eV, which is about that usually obtained for the other sintered samples.

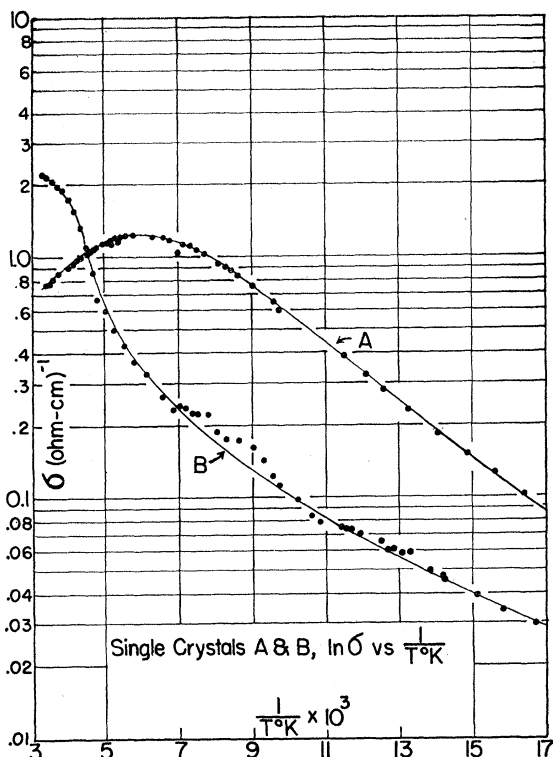


FIG. 6. Single crystals *A* and *B*, conductivity vs $1/T^{\circ}\text{K}$. The conductivity of this crystal is also similar to a polycrystalline sample.

For T between 90°K and 200°K , an activation energy about twice this appears. Because of the inability to obtain Hall effect curves and the sometimes deceptive nature of conductivity, no analysis of these curves is attempted except to say that because of apparent similarity in the conductivity curves we might imagine that the anomaly in the mobility behavior in crystal *B* may be present in this sample and may be characteristic of the zinc oxide rather than grain boundaries; i.e., crystal *B* may have had a more radical heat treatment. The room temperature measurements throw some doubt on the most usual concept of the zinc-oxide donor atom, that of the frozen-in interstitial zinc atom. On this model we might expect that the samples receiving this more drastic cooling treatment would have a higher conductivity and lower Hall coefficient, contrary to what is experimentally found.

III. DISCUSSION

1. Hall Effect and Applicable Models

In this section the results of the Hall-effect measurements are considered in some detail. The samples to which this part of the discussion applies have been sintered at temperatures ranging from 950°C to 1350°C for a period of 18 hours and quenched at temperatures of 600°C and lower. These measurements were reproducible, and no time effects were observed in the

samples where the electrical properties have been analyzed.

An interpretation of these measurements is sought in the light of existing semiconductor theory. Starting with the simple Wilson semiconductor model, the data are compared with a series of semiconductor models that could possibly apply. It is found that three distinct physical models can give a satisfactory interpretation of the experimental results.

A. Disagreement with Wilson Semiconductor Model

If we consider the usual simple Wilson semiconductor model for an n -type semiconductor,²² we have as shown in Fig. 1, a single impurity level at an energy E_D below the conduction band. (In all that follows the energy zero will be taken at the bottom of the conduction band.) E_G is the intrinsic energy gap, the distance between the top of the filled band and the bottom of the conduction band. It is large enough so that we can ignore the contribution of electrons made to the empty band by the filled band.

The equation for the number of electrons in the conduction band n is given by

$$n = (2N_D)^{1/2} \{2\pi mkT/h^2\}^{3/2} \exp\{-E_D/2kT\}, \quad (\text{III-1})$$

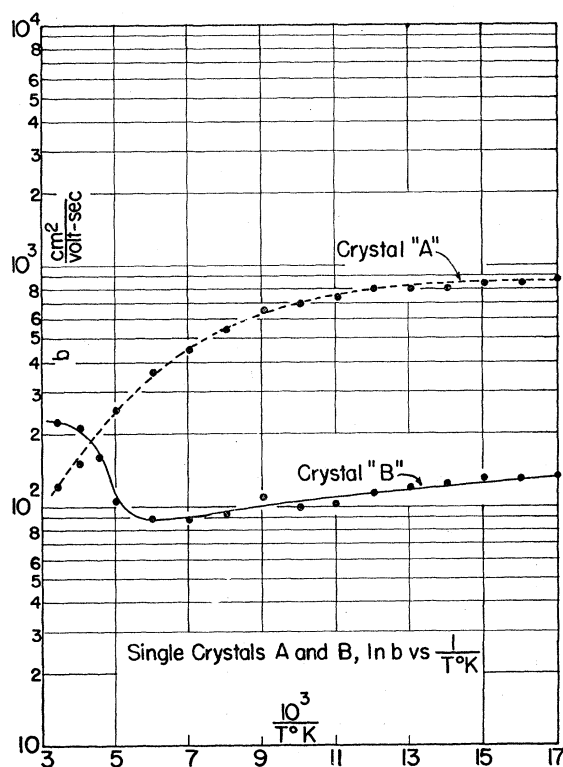


FIG. 7. Single crystal mobilities. Crystal *A* is similar to the moderate heat treatment samples, while crystal *B* exhibits an anomaly in the temperature behavior of its mobility.

²² F. Seitz, *The Modern Theory of Solids* (McGraw-Hill Book Company, Inc., New York, 1940), p. 186.

where N_D = number of donors/cm³. It should be kept in mind that (III-1) holds true only when most of the donor atoms are not ionized (for low temperatures). Each impurity atom is assumed in this model to have one electron available for excitation to the conduction band. The expression for the number of states in the conduction band, the Zn 4s band, is taken to be a parabolic function of the wave number. Also, m is considered to be the free-electron mass due to the fact that the conduction band is the broad 4s band of the Zn⁺⁺ ion.

We would expect then for a plot of $\ln(n/T^3)$ vs $1/T$ that we should obtain a straight line at low temperatures. Experimentally such a straight line is obtained as shown in the lower curve of Fig. 9, where we have plotted the results for sample No. 3. If this theory is correct, we should be able to derive a value of N_D from the intercept $(2N_D)^{1/2} (2\pi mk/h^2)^{3/2}$ of the straight line portion extrapolated back to the ordinate axis. This value should equal the number of carriers measured in the saturation region. The value at N_D obtained from the intercept appears, however, to be approximately 1/10 to 1/20 of n (saturation).

Graphically the essential feature of this result is that the straight portion of the experimental curve, and most of the region for which Eq. (III-1) is not valid ($n \sim N_D$),

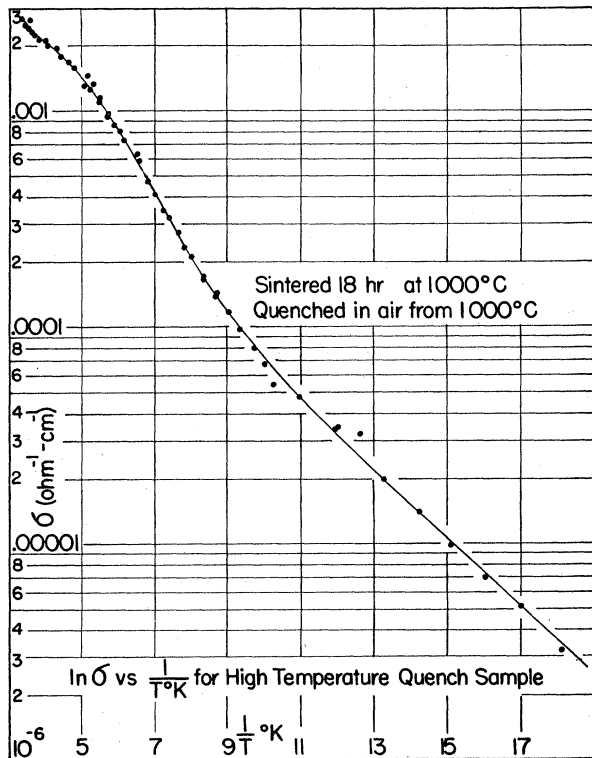


FIG. 8. Conductivity of a polycrystalline sample quenched in air from its sintering temperature. This sample is unlike those of moderate treatment and the curve may be compared with that of Crystal B.

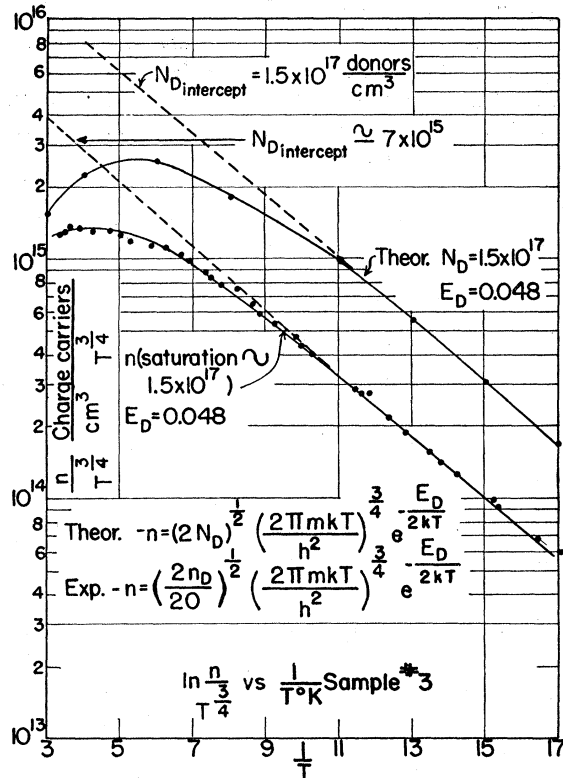


FIG. 9. Comparison of theoretical curve having the orbital degeneracy $D=20$ with the simple theory and experimental results. A value of orbital degeneracy of 20 fits experimental results quite well.

is displaced downward from a curve plotted for the single-level semiconductor model. This is shown in Fig. 9. The theoretical curve is plotted using the value of n (saturation) for the value of N_D , and the activation energy is taken to be $2k$ times the slope of the experimental plot of $\ln(n/T^3)$ vs $1/T$. The comparison of the curves indicates that the experimental curve could be fitted by using the parameter $N_D/20$ instead of N_D . This characteristic applies to all results, and the factor that serves to reduce the "effective" number of donors in Eq. (III-1) we will designate as D .

There are several additions or modifications that can be made to the Wilson semiconductor model. We shall discuss here three of those that satisfactorily account for the discrepancy between experiment and theory.

B. Orbital Degeneracy of the Impurity Level

Serin²³ has investigated the spectrum of an electron revolving around an impurity atom as exemplified by phosphorus in silicon (or a hole and aluminum in silicon). If the electron bound to the donor has an elliptical path, Serin's results indicate that the energy levels are degenerate. In regard to elliptical orbits, it is

²³ B. Serin, Technical Report No. 4, University of Pennsylvania, U. S. Bureau of Ships Contract, June 30, 1946 (unpublished).

found²⁴ that the crystalline fields in ZnO are such that the orbits of the valence electrons are stretched out along the c axis of the crystal. From electron diffraction results, Johnson²⁵ has found that the intensity of the diffraction lines can be matched only by an elliptical distribution of valence electrons with the ratio of the axes of this ellipse ~ 6 , with the major axis along the c axis. It should be pointed out that a tighter binding along the c axis is indicated because the ratio of c/a is 1.60 instead of 1.633 for an ideal hexagonal close-packed crystal.

If we use this degeneracy factor D , we are essentially stating that an electron bound to a donor can have any one of D orbits. It should be apparent that for the sake of electrical neutrality only one electron is allowed at each donor site and that once an electron occupies one orbit, the other $D-1$ orbits are unavailable for occupation. Setting this D factor into the statistics we find that the number of electrons in the donor level is given by

$$n_D = \frac{1}{1 + D^{-1} \exp\{-(E_D - \mu/kT)\}}, \quad (\text{III-2})$$

where the Fermi distribution has been modified by a factor $1/D$ multiplying the exponential term. μ is the Fermi energy.

Equation (III-1) will now become

$$n = \left(\frac{2N_D}{D}\right)^{\frac{3}{2}} \left\{ \frac{2\pi mkT}{h^2} \right\}^{\frac{3}{2}} e^{-E_D/2kT}.$$

Now the plot of $\ln(n/T^{\frac{3}{2}})$ for Eq. (III-3) will always fall below the plot of Eq. (III-1) and give a smaller value of the intercept N_D . Agreement with the experimental results is found if D is taken ~ 10 to 20 .

In the case of ZnO, an intuitive feeling as to what the degeneracy factor might mean can be obtained, if we consider the case of the interstitial zinc atom with its two valence $4s$ electrons. The interaction between the Zn^{++} ion and the electrons is reduced by $1/K^2$ (K represents the effective dielectric constant), and the difference between each level of the $n=4$ shell is then reduced, bringing the levels rather close together. We might then obtain an admixture of states for the $n=4$ shell.

C. Models with Traps

Other interesting physical cases can be built up, if we consider impurities or lattice defects in the crystal that do not have electrons available for excitation to the conduction band. These traps can lie at the donor level, below the donor level, or above the donor level. The first two trap positions correspond to the second and third models giving possible explanations of results.

a. N_T traps at the impurity level.—The number of electrons in the conduction band at any temperature is given by²⁶

$$n(N_T + n)/N_D - n = 2\{2\pi mkT/h^2\}^{\frac{3}{2}} e^{-E_D/kT}. \quad (\text{III-4})$$

For $n \ll N_T$, low temperatures, this expression becomes

$$n = (N_D/N_T) 2\{2\pi mkT/h^2\}^{\frac{3}{2}} e^{-E_D/kT}. \quad (\text{III-5})$$

For $n \gg N_T$, high temperatures, with $n \ll N_D$ we have

$$n = (2N_D)^{\frac{3}{2}} \{2\pi mkT/h^2\}^{\frac{3}{2}} e^{-E_D/2kT}. \quad (\text{III-6})$$

Note that these two curves give different slopes. At first sight we might reject the applicability of Eqs. (III-5) and (III-6) since we do not have two slopes in our experimental curves. Equation (III-6) is the same as (III-1). However, if we make $N_T \gg N_D$, then (III-6) is no longer valid and Eq. (III-5) holds over the entire temperature range where $n \ll N_D$. Equation (III-5) is capable of giving a proper value to the intercept. The intercept of the $\ln(n/T^{\frac{3}{2}})$ vs $1/T$ plot is $N_D/N_T (2\pi mk/h^2)^{\frac{3}{2}}$. Then for n (saturation) $= 2 \times 10^{17}$ electrons/cm³, N_T is approximately 8×10^{18} traps/cm³. Thus, with an extremely large number of traps at the impurity we are able to obtain a theoretical curve matching experimental results. This arrangement with $N_T \gg N_D$ we refer to as the second scheme.

b. N_T traps below the impurity level.—A third scheme that will give satisfactory interpretation of our data is that of N_T low-lying traps per cm³, such that the number of available electrons is $N_D - N_T$. This is mathematically identical (we have merely substituted $N_D - N_T$ for N_D) to the trap scheme just mentioned, but we keep this as a distinct mechanism, because of the fact that the actual physical models considered in the next section are not similar.

Some evidence for this two-level energy scheme may be found in Miller's results for conductivity.¹⁴ Miller's conductivity curve indicates the possibility of two saturation regions. The low-temperature slope in Miller's work is 0.02 ev, whereas the high-temperature slope is 0.7 ev. The 0.7-ev slope may be identified with elevation of electrons from the trap levels to the conduction band.

In Fig. 10 we have compared logarithmic plots of the various models. Curve *A* represents a $\ln(n/T^{\frac{3}{2}})$ vs $1/T$ plot of the simple model with $N_D = 10^{17}$ donors/cm³ and $E_D = 0.05$ ev. Curve *B* represents the same type of plot as *A*, but now we have added a degeneracy factor of ten. Curve *C* represents a $\ln(n/T^{\frac{3}{2}})$ plot of the same values of n as one finds in the curve *B*. This plot corresponds to a model of 2.9×10^{18} donors/cm³ with an activation energy of 0.021 ev and 2.8×10^{18} low-lying traps/cm³. A degeneracy of 10 with $N_D = 10^{17}$ donors/cm³ corresponds to $N_D = 2.9 \times 10^{18}$ donors/cm³ for a low-lying trap model. The model consisting of donors and

²⁴ C. H. Erhardt and K. Lark-Horowitz, Phys. Rev. **57**, 603 (1940).

²⁵ V. A. Johnson, Phys. Rev. **57**, 613 (1940).

²⁶ N. Mott and R. Gurney, *Electronic Processes in Ionic Crystals* (Oxford University Press, London, 1948), p. 159; B. R. Nijboer, Proc. Phys. Soc. (London) **51**, 505 (1939); J. H. DeBoer and W. C. Van Geel, Physica **2**, 286 (1935).

traps at the same level would also correspond to curve C if $N_D = 10^{17}$ donors/cm³, $N_T = 2.8 \times 10^{18}$ traps/cm³, and $E_D = 0.021$ ev.

It is necessary to note that the discrepancy in N_D (intercept) can be satisfactorily accounted for if we use a value for the electron mass of about 1/7 that of a free electron. There is, as far as we can determine, no reason to expect that the mass of a conduction electron should be so small.

Traps above the donor level will give a value of N_D (intercept) that is too large,²⁷ and hence we will not discuss this scheme further.

IV. PHYSICAL MODELS FOR THE IMPURITY CENTER

In this section we examine the possibilities for the physical realization of the impurity energy level models that we have discussed earlier. We consider first the centers to which other authors have attributed the properties of ZnO and how they fit our experimental results. Several modifications and additions to these earlier proposals are discussed in the light of recent work on alkali halides and other ionic crystals. It is suggested that perhaps the best physical model is a pair of negative and positive ion vacancies with unpaired negative ion vacancies in the lattice when there is a stoichiometric excess of the metallic constituent.

For pure metallic oxide semiconductors with a stoichiometric excess of the metallic component we have two simple possibilities for lattice defects: interstitial metal atoms or oxygen ion vacancies. Either one would indicate an increase in the lattice constant as is experimentally found by x-ray diffraction. Mott and Littleton²⁸ have shown that the lattice expands around a chloride vacancy in NaCl. It is then reasonable to expect a similar result for anion vacancies in ZnO. The actual physical density would increase for interstitials and decrease for vacancies. No density changes have been measured in semiconducting ZnO.

Wagner²⁹ has dismissed the possibility of negative ion vacancies in the ZnO lattice by demonstrating that the negative ion transport number is very small compared with that of the positive ion transport number. However, in the case of KCl, where again the positive transport number is much larger than that of the negative ion, Seitz³⁰ has assumed that the negative ion vacancies move about under thermal agitation in the company of positive ion vacancies since such pairs of vacancies are much more mobile than the negative ion vacancies themselves. Dienes and Seitz³¹ have calculated the activation energy for a pair of vacancies of KCl to be about 0.38 ev. The experiments of Leivo,

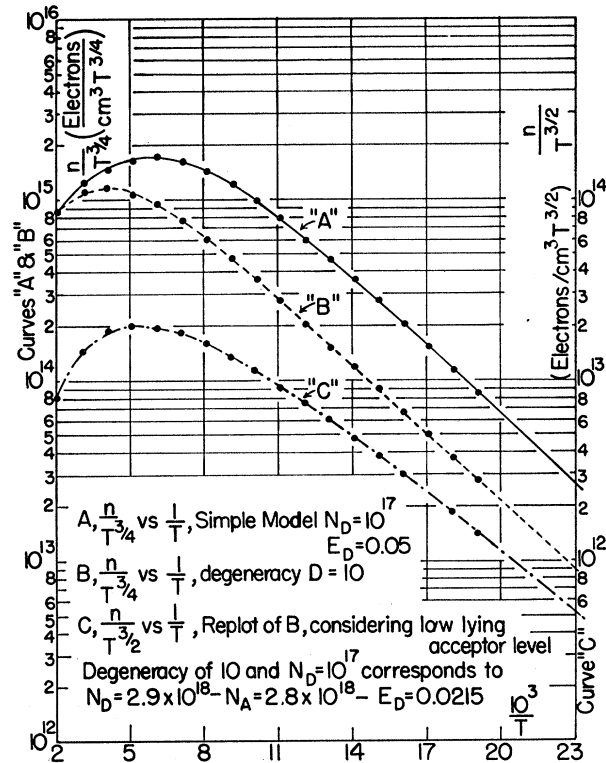


Fig. 10. Comparison of the various semiconductor models. Curve A represents the simple Wilson model. Curve B is the orbital degeneracy model with $D=10$. Curve C is the low-lying trap model that gives the same intercept value of available electrons and temperature variation of n as Curve B.

Estermann, and Stern³² show that vacancies diffuse into the lattice at room temperature at a rate such that the activation energy of this migration is of the order of 0.5 ev. This pair of vacancies is considered to eject a positive ion vacancy on the capture of an electron to form an F center. Diffusion of pairs of vacancies may then also be considered in the formation or production of the semiconducting ZnO.

DeBoer and Verwey³³ have assumed that the impurity centers in some metallic oxides are oxygen vacancies. Experimental evidence for this is found in BaO (NaCl structure). Their arguments cannot be extended unambiguously to ZnO because of the greater polarizability of zinc and the different lattice structure.

It should be pointed out that the possibility of interstitial positive ions in the case of alkali halides has been eliminated by the calculations of Mott and Littleton.²⁸ We might expect, however, that the wurtzite structure of ZnO would be somewhat more amenable to the positioning of a metallic ion in an interstice of the lattice.

Since at the present time we cannot rule out either the interstitial zinc atom or the oxygen ion vacancy,

²⁷ S. E. Harrison, thesis (unpublished).

²⁸ N. F. Mott and M. J. Littleton, *Trans. Faraday Soc.* **34**, 485 (1938).

²⁹ C. Wagner, *Z. physik. Chem.* **22B**, 181 (1933).

³⁰ F. Seitz, *Revs. Modern Phys.* **18**, 384 (1946).

³¹ G. J. Dienes and F. Seitz, *Phys. Rev.* **73**, 1260 (1948); G. J. Dienes, *J. Chem. Phys.* **16**, 620 (1948).

³² Leivo, Estermann, and Stern, *Phys. Rev.* **75**, 627 (1949).

³³ J. H. DeBoer and E. J. Verwey, *Proc. Phys. Soc. (London)* **49**, 57 (1937) (Extra part).

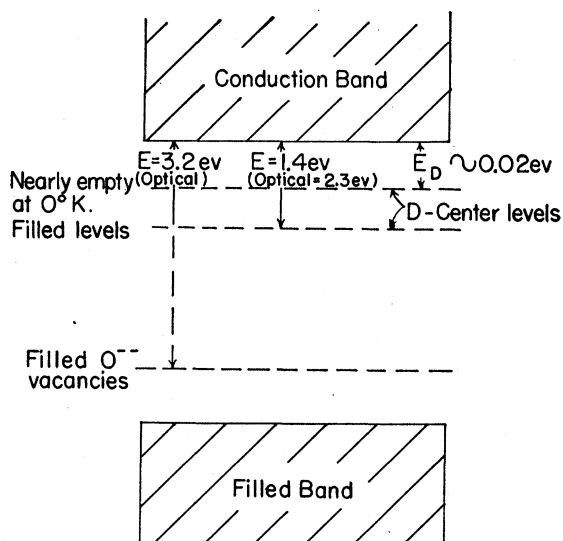


FIG. 11. *D*-center model with excess oxygen vacancies. The thermal and optical activation energies that have been obtained experimentally are shown with the levels to which they correspond.

we have examined these defects with the purpose of suggesting a different physical model to describe each of the three methods of interpreting the Hall effect curves discussed in Sec. III, and to determine which of these is physically the most satisfactory.

We begin with the discussion of the orbital degeneracy model.

An interstitial zinc atom is very amenable to the treatment of degeneracy. The polarizability of the interstitial zinc atom in its anisotropic surroundings and the elliptical distribution of the valence electrons found from electron diffraction would both produce the elliptical orbits of the electrons on the interstitial zinc atom, mentioned in Sec. III-1. The wave functions necessary to describe these orbits would have *p* and *d* states and, therefore, be highly degenerate.

For the second energy scheme consisting of N_D donors and N_T traps at the same level, we may postulate the existence of oxygen vacancies, with the excess zinc playing a similar role as the alkali metal in a halide crystal that has been heated in an atmosphere of the metal. The final number of negative ion vacancies, then, is roughly the sum of those originally present in the ZnO lattice, which satisfy the conditions of statistical equilibrium at stoichiometric equality, and those which are produced by the excess zinc atoms (actually the loss of oxygen). In other words, we have normally about 10^{18} zinc and oxygen vacancies and about 10^{17} excess zinc ions, using the experimental data of Sec. III-1-C. This model is subject to doubt in the light of Pincherle's³⁴ calculations of the activation energy of two electrons bound to a negative ion vacancy. He has calculated the binding energy of the outer electron to

be 2.7 eV for PbS (cubic) crystal. It is interesting to note that the same author has shown for this type center that the energy of the electrons attached to the negative ion vacancies is not inversely proportional to the square of the dielectric constant, with the subsequent result that the radii of these electron orbits are smaller than those of the hydrogen atom times the dielectric constant.³⁵ The overlapping of these orbits has been put forward as one explanation for the variation of the activation energy with impurity content. This variation is for the most part absent in our ZnO samples.

We now examine the third energy model of donors and low-lying traps.

Before the existence of this model we had considered only the simple defects, interstitial zinc atoms and oxygen ion vacancies. We may take up the concept of pairs of vacancies and consider the pair itself as the impurity center. With this idea in mind, a model for low-lying traps is suggested by Pincherle's³⁴ treatment of the case of a positive and negative ion vacancy pair (this is designated as *D* center by Pincherle) which can accept up to two electrons. He finds the binding energy of the second electron to be close to zero and the second ionization energy is of the order of 0.25 eV. The first ionization energy could correspond to the 0.025 eV activation energy and the second to 1.4 eV found from the high temperature measurements. As shown in Sec. III, the first activation energy is taken to be directly equal to the slope of a semi log plot, while the second activation energy is that from a level of completely filled traps and, therefore, is twice the slope. It is implied that the upper levels are only partially occupied due to an inadequate supply of electrons caused by a still lower set of traps as illustrated in Fig. 11 and explained below. Though good quantitative agreement is lacking between this model and Pincherle's calculations, it should be pointed out that his work is done for cubic PbS and is admittedly rough. For our purposes the important qualitative feature is the existence of two levels and widely dispersed activation energies as compared with the first and second ionization energies of a Coulomb potential.

Further corroborating evidence for the *D* center can be found in the explanation of other properties of ZnO by means of this physical model. First it will be necessary to realize that it has been demonstrated experimentally⁴ for polycrystalline samples, and is now generally assumed, that the ZnO semiconductor contains an excess of zinc. When this is the case, we postulate that accompanying the formation of *D* centers (positive plus negative ion vacancies) there exists in the lattice network an excess of unpaired oxygen ion vacancies which will form additional deep-lying levels (>1.4 eV). Thus, the impurity level scheme consists of a very low-lying oxygen ion vacancy containing two electrons with two higher *D*-center levels. The lower

³⁴ L. Pincherle, Proc. Phys. Soc. (London) **A64**, 650 (1951).

³⁵ L. Pincherle, Proc. Phys. Soc. (London) **A64**, 664 (1951).

D-center level is completely filled, whereas the upper *D*-center level is almost completely empty. Then most of the electrons of the excess zinc are divided between the levels of the oxygen ion vacancies and the lower *D*-center levels.

It is apparent that if we used a model of only pairs of vacancies and excess oxygen vacancies, the *D*-center levels would not contain any electrons. However, the distribution of electrons among the *D* centers and excess oxygen vacancies necessary to describe experimental results may arise in one of several ways. The excess zinc could take up interstitial as well as lattice points.³⁶ Also, the electrons active in *D* centers are possibly contributed in a large part by the impurities in the spectroscopically pure powder.

Now we can associate the luminescence peak arising at 5100Å (2.3 eV) with the transition from an excited state lying near the conduction band to the lower energy level of the *D* center. This discrepancy between the thermal and optical activation energies is certainly reasonable, as has been pointed out by Mott and Gurney³⁷ and by DeBoer and Van Geel.³⁸ The luminescence peak at 3950Å (3.2 eV) may be assumed to be a transition from an excited state near the conduction band to an oxygen vacancy. Pincherle's value for a similar transition in lead sulfide to a sulfur ion vacancy is 2.7 eV. Further, the temperature variation³⁹ of magnitude and shape of the intensity *vs* wavelength curve of the 3900Å luminescence peak represents that of an ensemble of individual centers such as that obtained from *F* centers.³⁰ The peak moves toward longer wavelengths and broadens with increasing temperature. The 5100Å peak also broadens,³⁹ but its wavelength remains fixed as the temperature increases. The ultraviolet peak is much narrower than the green peak, which has the diffuse character of that of the bands in the alkali halides which Seitz has associated with centers containing more than one vacancy.

It has been found that the ultraviolet peak is missing in the luminescent spectrum of single crystals. In this case, we postulate that in our single crystals the excess of zinc is so small that for our measurements all oxygen ion vacancies are paired with zinc ion vacancies. The electrons for the *D* centers can be donated by the foreign impurity atoms which are obviously present in our single crystals. Then in single crystals we still obtain the 0.025-eV slope at low temperatures because of the presence of *D* centers, though we have no excess zinc. (See Fig. 6.)

Heretofore, the impurity center has most often been assumed to be "frozen-in" interstitial zinc. However, quenching from high temperatures apparently does not

produce more impurity centers, but it does decrease the conductivity and increase the Hall effect. At temperatures below 100°K the high-temperature quenched samples demonstrate the slope associated with *D* centers. At these high temperatures of quenching the *D* centers are probably mostly dissociated and, therefore, the fraction of single Zn⁺⁺ and O⁻⁻ ion vacancies is increased by the high temperature quenching.⁴⁰

It is, of course, obvious that we have not exhausted the supply of possible physical models, but those we have discussed will suffice to supply physical interpretation of the energy schemes used in Sec. III to analyze the Hall effect curves.

Considering now all of the physical models, we are inclined to favor the *D* centers with accompanying oxygen ion vacancy because of its ability to explain other properties as well as those that we have measured.

V. SUMMARY

The Hall effect and conductivity have been measured and analyzed in the temperature range from 54°K to 300°K for sintered samples of moderate heat treatment and two single-crystal specimens. The Hall effect curves of all of these specimens indicate the same slope for a $\ln R$ *vs* $1/T$ plot. This same slope was observed in the conductivity curves of these sintered specimens and one of the single-crystal specimens, demonstrating that our results are probably characteristic of the bulk ZnO and not subject to the disguising influences of grain boundary effects.

Analysis of the Hall coefficient curves leads to three energy level schemes: (1) donor centers with degenerate levels, (2) traps at the donor level, and (3) traps lying far below the donor level. The preferred physical model is *D* centers (paired zinc and oxygen vacancies) plus excess oxygen vacancies, considering, in addition, properties of ZnO other than those measured by the paper and this corresponds to model (3) above.

The mobilities of the sintered samples, as defined by a product of the conductivity σ and Hall effect R all have the same temperature dependence but vary in magnitude from sample to sample.

The single-crystal mobilities are, naturally, the largest. The mobility of one crystal has the same temperature dependence as these sintered samples, while the second crystal exhibits a rather anomalous behavior. The conductivity curve of the second crystal resembles that of samples that have been given a more radical heat treatment (higher temperature of quenching).

⁴⁰ A. B. Scott and L. P. Bupp [Phys. Rev. **79**, 341 (1950)] have found that there exists an equilibrium between *F* centers and aggregates of defects containing electrons in KCl. These aggregates tend to form if the KCl crystal is cooled slowly. In KCl the aggregates are more stable than *F* centers below 300°C, whereas at temperatures above 500°C the *F* centers are more stable. At intermediate temperatures there exists a thermal equilibrium between *F*-centers. Note added in proof: the dissociation energy for paired vacancies is 0.89 eV as calculated by J. R. Reitz and J. L. Gammel, J. Chem. Phys. **19**, 894 (1951).

³⁶ The distribution of the excess atoms between lattice and interlattice points is discussed by R. H. Fowler and E. H. Guggenheim, *Statistical Thermodynamics* (Cambridge University Press, Cambridge, 1949), Chap. 13.

³⁷ N. Mott and R. Gurney, reference 26, p. 264.

³⁸ J. H. DeBoer and W. Ch. Van Geel, *Physica* **2**, 286 (1935).

³⁹ F. H. Nicoll, *J. Opt. Soc. Am.* **38**, 178 (1950).

These results suggest that the conductive process are influenced by quenching from a temperature somewhere above 600°C. All of our "moderately" heat-treated samples have been quenched at this and lower temperatures. If both Hall effect and the conductivity of samples quenched from temperatures between 600°C and 1100°C can be measured, then we should be able to determine at which temperatures these "anomalous" conduction mechanisms appear and perhaps gain some insight into the temperature of formation or dispersion of some of the impurity centers mentioned in Sec. IV.

An infrared photoconductivity experiment at liquid helium temperatures could decide between the first model and the last two, while a photoconductivity experiment at shorter wavelength to establish the existence of traps could eliminate the second or third. Thermoluminescent curves of samples heated from liquid helium temperatures after irradiation with ultraviolet light should also add some information on the shallow impurity levels of the physical models suggested in Sec. III for each of these energy schemes.

High-temperature Hall effect and conductivity measurements should certainly shed some light on the mechanism of the *D*-center formation. At temperatures at which the *D* centers might start to dissociate into positive and negative ion vacancies, the Hall coefficient should rise due to the capture of two electrons by each oxygen ion vacancy. The effect on conductivity may or may not be masked due to the possible exponential change of mobility with temperature. Further, on heating to temperatures that are high enough to dis-

sociate the *D* center and quenching to temperatures that are low enough to prevent diffusion, we should be able to vary the concentration of *D* centers. This would affect both Hall and conductivity measurements at low temperatures. The destruction of *D* centers with the increase of oxygen ion vacancies should diminish the intensity of the green luminescence while enhancing the output of the ultraviolet peak.

The existence of two, lattice vacancies of opposite sign side by side could be detected by a peak in the variation of the dielectric loss constant as a function of frequency similar to that reported by Breckenridge⁴¹ for the alkali halides. This frequency would correspond to the jump frequency of the pairs of vacancies.

Experiments just mentioned may help decide whether the *D*-center model is applicable. Alternatively, they may suggest that we need a more complex impurity system to explain all of the effects of ZnO or that the bulk effects that we have measured are not associated with centers that produce the other effects discussed.

ACKNOWLEDGMENT

The author wishes to express his appreciation to Professor P. H. Miller, Jr., for his guidance and encouragement through the entire course of the work. He is also greatly indebted to Professor G. R. Russel for many valuable discussions and suggestions. Many thanks are due Mr. A. Nussbaum and Miss L. Y. Lynn for their assistance with the experimental details.

⁴¹R. G. Breckenridge, *J. Chem. Phys.* **16**, 959 (1948); **18**, 913 (1950).

Lattice-Scattering Mobility in Germanium

F. J. MORIN

Bell Telephone Laboratories, Murray Hill, New Jersey

(Received September 16, 1953)

The temperature dependence of lattice-scattering mobility in germanium is determined from conductivity. It is found to be $T^{-1.66}$ for electrons and $T^{-2.33}$ for holes. The result for holes suggests that the valence band is not at the center of the Brillouin zone. The ratio Hall mobility/conductivity mobility is also determined. It is found to be constant with temperature at ~ 1.05 for electrons. The ratio for holes shows significant temperature dependence. This suggests that the valence band is composed of multiple surfaces of minimum energy.

THE temperature dependence of lattice-scattering mobility in germanium has been reported¹⁻⁵ as being different from the theoretically predicted $T^{-1.5}$: in general, it is found to be $T^{-1.6}$ for electrons and $T^{-2.3}$ for holes. These results have theoretical significance since the prediction $T^{-1.5}$ assumes the band edge to be located at the center of the Brillouin zone. In the references cited above, the temperature dependence of

lattice-scattering mobility was determined from conductivity and drift or Hall mobility. In this note, it is determined from conductivity. This method has some advantage over the others since drift measurements are more difficult and perhaps less precise, and Hall results will be misleading if the ratio of Hall mobility to conductivity mobility is a function of temperature.

The ratio Hall mobility/conductivity mobility, μ_H/μ , as a function of temperature has also been determined. The magnitude and temperature dependence of this ratio has theoretical significance with regard to the shape and number of the surfaces of minimum energy

¹W. C. Dunlap, *Phys. Rev.* **79**, 286 (1950).

²M. B. Prince, *Phys. Rev.* **91**, 208 (1953).

³R. Lawrence, *Phys. Rev.* **89**, 1295 (1953).

⁴P. P. Debye and E. M. Conwell (to be published).

⁵L. P. Hunter, *Phys. Rev.* **91**, 579 (1953).